

Isozyme-Specific Transition State Inhibitors for the Trypanosomal Nucleoside Hydrolases[†]

David. W. Parkin,^{‡,§} Gerrit Limberg,^{||} Peter C. Tyler,^{||} Richard H. Furneaux,^{||} Xiang-Yang Chen,[‡] and Vern L. Schramm^{*,‡}

Department of Biochemistry, Albert Einstein College of Medicine of Yeshiva University, 1300 Morris Park Avenue, Bronx, New York 10461, and Industrial Research Limited, Lower Hutt, New Zealand

Received September 16, 1996; Revised Manuscript Received January 23, 1997[®]

ABSTRACT: Protozoan parasites lack de novo purine biosynthesis and require purine salvage from the host. Nucleoside hydrolases are involved in nucleoside salvage and are not found in mammals, making them protozoan-specific targets for inhibitor design. Several protozoan nucleoside hydrolase isozymes with distinct substrate specificities have been characterized. Novel substituted iminoribitols have been synthesized to resemble the transition state structure of the nonspecific inosine–uridine nucleoside hydrolase from *Crithidia fasciculata* (IU-nucleoside hydrolase). These inhibitors have been characterized for this enzyme and for a purine-specific nucleoside hydrolase (IAG-nucleoside hydrolase) from *Trypanosoma brucei brucei*. Inhibitors which provide nanomolar inhibition constants for IU-nucleoside hydrolase exhibit micromolar inhibition constants for the IAG-enzyme. For example, *p*-bromophenyliminoribitol inhibits the IU- and IAG-enzymes with dissociation constants of 28 nM and 190 μ M, respectively. Substrate specificity, the action of transition state inhibitors and the pH-dependence of the kinetic constants establish that the catalytic mechanisms and transition state structures are fundamentally different for the IU- and IAG-isozymes. The finding is remarkable since these isozymes share significant homology at the catalytic sites and both use inosine as a preferred substrate. The specificity of the transition state analogues indicates that logically-designed transition state inhibitors are isozyme-specific, with (K_m/K_i IU-nucleoside hydrolase)/(K_m/K_i IAG-nucleoside hydrolase) values up to 39 000. The mechanism of the differential inhibition is based on the relative leaving group activation and ribosyl–oxocarbenium-forming abilities of these enzymes. In addition to providing isozyme-specific inhibitors, the novel molecules described here have diagnostic value for the nature of the transition states for *N*-ribohydrolase enzymes.

Nucleoside *N*-ribohydrolases are enzymes found in prokaryotes and unicellular eukaryotes which release purine and pyrimidine bases from their nucleoside sugars for salvage by phosphoribosyltransferases (Dewey & Kidder, 1973; Miller et al., 1984). The purine salvage pathways are essential in the parasites, since the organisms have lost the capacity for de novo purine biosynthesis and rely completely on salvage pathways for their precursors of RNA and DNA synthesis (Hammond & Gutteridge, 1984). These organisms are estimated to infect more than 2 billion persons worldwide and are thought to claim over two million lives per year, primarily infant mortalities from malaria (Miller, 1992). Important features of these enzymes are that none is known to exist in mammalian cells (Gopaul et al., 1996) and that they are the primary pathway for nucleoside salvage, at least in the few organisms whose pathways of nucleoside salvage have been characterized (Estupiñán & Schramm, 1994). These features make the protozoan nucleoside hydrolases significant enzymes as targets for logical inhibitor design (Schramm et al., 1994). In previous work, the IU-nucleoside

hydrolase¹ from *Crithidia fasciculata*, a trypanosome which resides in mosquitoes but is not parasitic for mammals, was characterized by kinetic isotope effects and transition state analysis. The results have led to the ability to logically design chemically varied inhibitors which act as transition state analogues based on their (1) electrostatic similarity to the transition state structures (Horenstein & Schramm, 1993a,b), (2) responses in K_i to pH, (3) tight-binding inhibition leading to K_m/K_i values of 10^5 – 10^6 , (4) nanomolar inhibition constants, and (5) distortion toward transition state charge and geometry when bound to the enzyme (Parkin & Schramm, 1995; Boutellier et al., 1994; Deng et al., 1996).

A comparison of the nonspecific IU-nucleoside hydrolase with two isozymes specific for purine nucleosides indicated that the isozymes differ in their affinity for transition-state analogues and in their ability to cleave a chromophoric substrate, nitrophenylribose (Estupiñán & Schramm, 1994; Mazzella et al., 1996; Parkin, 1996). In this study the (*S*) substituted² iminoribitol inhibitors were varied in the substituent which occupies the enzymatic binding sites for the

[†] This work was supported by Research Grants GM41916 and AI34342 from the National Institutes of Health and from the G. Harold and Leila Y. Mathers Charitable Foundation.

* To whom correspondence should be addressed. Tel: (718) 430-2813. FAX: (718) 430-8565. E-mail: vern@aeom.yu.edu.

[‡] Albert Einstein College of Medicine of Yeshiva University.

[§] Current address: International Livestock Research Institute, Nairobi, Kenya.

^{||} Industrial Research Limited.

[®] Abstract published in *Advance ACS Abstracts*, March 15, 1997.

¹ Abbreviations: IU-nucleoside hydrolase, the inosine and uridine utilizing, nonspecific nucleoside hydrolase from *Crithidia fasciculata* (Parkin et al., 1991); IAG-nucleoside hydrolase, the inosine, adenosine, and guanosine utilizing, purine-specific nucleoside hydrolase from *T. brucei brucei* (Parkin, 1996); nitrophenylribose, *p*-nitrophenyl β -D-ribofuranoside; iminoribitol, 1,4-dideoxy-1,4-imino-D-ribitol (see I in Table 1); phenyliminoribitol, 1-(*S*)-phenyl-1,4-dideoxy-1,4-imino-D-ribitol (see V in Table 1).

purine base of substrates. The family of inhibitors was tested with two distinct isozymes characteristic of the trypanosomal *N*-ribohydrolases.

The IU-nucleoside hydrolase from *Crithidia* catalyzes the hydrolysis of all of the commonly occurring purine and pyrimidine nucleosides. The kinetic mechanism is rapid-equilibrium random, has a relatively high K_m ($>100\ \mu\text{M}$ for inosine), is catalytically inefficient ($k_{\text{cat}}/K_m = 10^5\ \text{M}^{-1}\ \text{s}^{-1}$), and is strongly inhibited by ribo-oxocarbenium mimics (Parkin et al., 1991; Horenstein & Schramm, 1993a,b). These properties are compared to the IAG-nucleoside hydrolase, a purine-specific enzyme from *Trypanosoma brucei brucei*. *Trypanosoma congolense*, *T. vivax*, and *T. brucei brucei* are tsetse-transmitted parasites which cause trypanosomiasis in animals, while *T. brucei gambiense* and *T. brucei rhodesiense* cause sleeping sickness in humans. Although both the IU- and IAG-enzymes hydrolyze inosine to hypoxanthine and ribose, they exhibit different pH profiles and dramatically different sensitivity to the transition state inhibitor phenyliminoribitol with K_m/K_i values of 370 and 0.1 for the IU- and IAG-enzymes, respectively (Parkin, 1996). These results, together with site-directed mutagenesis and novel substrates, led to a mechanistic comparison of a family of five *N*-ribohydrolases and phosphorylases, with the conclusion that of these, the IU-nucleosidase was unique in obtaining the largest fraction of its catalytic potential from conversion of the ribosyl to the oxocarbenium transition state, while the others derived a larger fraction of the energy of activation from protonation or otherwise activating the purine leaving group (Mazzella et al., 1996; Gopaul et al., 1996). Leaving-group activation is also the mechanism for the acid-catalyzed solvolysis of *N*-ribosides, which occurs by diprotonation of the leaving group to form the purine dication prior to its departure (Garrett & Mehta, 1972). In contrast, base-catalyzed solvolysis (Handlon et al., 1994) is proposed to ionize ribosyl hydroxyl groups, and electrostatic stabilization mechanisms (Cherian et al., 1990) are proposed to favor conversion of the ribosyl moiety to the oxocarbenium ion character of the transition state.

The enzymatic mechanisms use a combination of ribosyl activation and leaving group activation, in which the contribution of the $\sim 18\ \text{kcal/mol}$ $\Delta\Delta G$ to lower the activation energy of the transition state barrier comes from a combination of conversion of the ribosyl toward the transition state and protonation of the leaving group as the mechanism for leaving group activation. The ability of nucleoside hydrolases to use nitrophenylribose as substrate and the mutation of the proposed leaving group proton donor has indicated that the IU-nucleoside hydrolase contributes $-4.6\ \text{kcal/mol}$ to leaving group activation and $-13.1\ \text{kcal/mol}$ to ribosyl activation (Mazzella et al., 1996; Gopaul et al., 1996). In the present study, the IAG-nucleoside hydrolase is found to lower the $\Delta\Delta G$ of activation by approximately $-9\ \text{kcal/mol}$ via leaving group activation and to also contribute approximately $-9\ \text{kcal/mol}$ to lowering transition state energy by ribosyl activation (see Discussion).

Effective transition state inhibitors of IU-nucleoside hydrolase are iminoribitols in β -linkage to a hydrophobic group provided by a phenyl ring, and a phenyl substituent which

can accept a hydrogen bond, or create an electron-rich hydrogen-bonding site, preferably in the *para*-position of the phenyl ring (see below). Inhibitors with these properties result in a binding energy approximately $-5\ \text{kcal/mol}$ more favorable than substrate. In contrast, the IAG-nucleoside hydrolase is not strongly inhibited by any of the available inhibitors with these properties. Only one of twelve inhibitors characterized here shows binding equal to or greater than the K_m for substrate. However, among this group, the best inhibitors are those which have phenyl substituents of hydroxyl and amino groups.

The unique inhibitors described here provide a new family of nanomolar inhibitors for the IU-nucleoside hydrolase and strengthen the hypothesis that this enzyme derives most of its transition state binding energy from interactions with the ribosyl group, while accepting most phenyl substituents in the aglycone. In contrast, the IAG-nucleoside hydrolase relies primarily on specific leaving group interactions for catalysis, and the monosubstituted phenyl group is incapable of capturing substantial energetic contributions from transition state interactions. This information is required for the synthesis of inhibitors for the purine-specific nucleoside hydrolases. On the basis of the results reported here, the nucleoside hydrolases are a class of enzymes in which isozyme-specific inhibition is possible. This approach has been valuable in the design of antibacterial agents. For example, dihydrofolate reductases from bacteria bind trimethoprin much more tightly than do the mammalian enzymes (Matthews et al., 1985).

MATERIALS AND METHODS

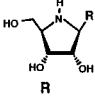
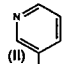
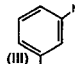
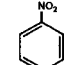
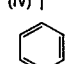
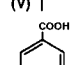
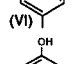
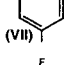
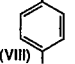
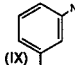
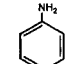
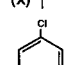
Enzymes. Inosine-uridine nucleoside hydrolase (IU-nucleoside hydrolase) was purified from extracts of *Escherichia coli* strain BL21(DE3)pLysS which contained the coding region for the enzyme isolated from *C. fasciculata* in a pET3d expression plasmid. The DNA coding for the enzyme was placed in the *NcoI*-*Bam*HI site. This construct gives a Pro2Ala substitution which has no significant effect on the kinetic properties of the purified enzyme. The overexpressed enzyme was purified to apparent homogeneity as previously described (Gopaul et al., 1996).

The IAG-nucleoside hydrolase was purified from the blood-stream form of *T. brucei brucei* (ILTaT 1.1) grown in sublethally irradiated (650 rads) Sprague-Dawley rats. The enzyme was purified to apparent homogeneity as determined by denaturing polyacrylamide gel electrophoresis (Parkin, 1996). Some of the studies used the *T. brucei brucei* enzyme which was overexpressed in *E. coli*.

Enzyme Assays. Initial rate measurements were accomplished at $30\ ^\circ\text{C}$ in reaction mixtures containing $50\ \text{mM}$ potassium phosphate, pH 7.5, or $50\ \text{mM}$ Hepes, pH 8.0, and nitrophenylribose or inosine as substrates (Mazzella et al., 1996). At pH 7.5 the product *p*-nitrophenylate anion is present at a concentration which gives a millimolar extinction coefficient of $9.3\ \text{cm}^{-1}$ at $400\ \text{nm}$. Reaction mixtures with nitrophenylribose as substrate were initiated by the addition of enzyme, and product formation was monitored by continuous recording at $400\ \text{nm}$. With inosine as substrate, the conversion to hypoxanthine was monitored continuously at $280\ \text{nm}$ (Parkin et al., 1991). The interactions of **I**, **V**, **VIII**, **XI**, and **XII** (see Table 1) with IU-nucleoside hydrolase were established to be slope-linear competitive inhibitors by measuring initial rates of product formation at a minimum

² The (*S*) stereochemistry at the 1-position of iminoribitol is equivalent to the β -anomeric position for ribose (Horenstein et al., 1993).

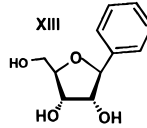
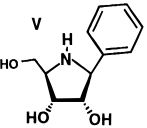
Table 1: Kinetic Constants for Inhibition of Nucleoside Hydrolases by Iminoribitols

|  | IU-nucleoside hydrolase ^a | | IAG-nucleoside hydrolase ^b | | K_m/K_i (IU-NH) K_m/K_i (IAG-NH) |
|---|--------------------------------------|-----------|---------------------------------------|-----------|---|
| | K_i | K_m/K_i | K_i | K_m/K_i | |
| (I) H | 4.5 ± 0.4 μM | 25 | 44 ± 4 μM | 0.41 | 60 |
| (II)  | 7.9 ± 0.6 μM | 14 | >240 ^c μM | <0.075 | >187 |
| (III)  | 7.5 ± 0.5 μM | 15 | >360 ^c μM | <0.05 | >296 |
| (IV)  | 1.1 ± 0.1 μM | 101 | >360 ^c μM | <0.05 | >2,000 |
| (V)  | 300 ± 27 nM | 370 | 180 ± 15 μM | 0.1 | 3,700 |
| (VI)  | 96 ± 7 nM | 1,160 | >480 ^c μM | <0.04 | >30,800 |
| (VII)  | 75 ± 4 nM | 1,480 | 35 ± 2 μM | 0.51 | 2,900 |
| (VIII)  | 57 ± 5 nM | 1,950 | 205 ± 14 μM | 0.088 | 22,180 |
| (IX)  | 51 ± 4 nM | 2,180 | 38 ± 4 μM | 0.47 | 4,590 |
| (X)  | 30 ± 2 nM | 3,700 | 12 ± 1 μM | 1.5 | 2,470 |
| (XI)  | 30 ± 1.4 nM | 3,700 | 190 ± 8 μM | 0.095 | 39,000 |
| (XII)  | 28 ± 4 nM | 3,960 | 113 ± 6 μM | 0.16 | 24,890 |

^a The K_m for inosine was 111 ± 17 μM under these assay conditions. K_m/K_i values are for inosine as substrate. Values for **I** and **V** are from Horenstein and Schramm (1993b). ^b The K_m for inosine was 18 ± 1 μM under these assay conditions. K_m/K_i values are for inosine as substrate. ^c No inhibition was observed at 80, 120, 120, and 160 μM **II**, **III**, **IV**, and **VI**, respectively, when assayed at 75 μM inosine. The indicated inhibitor constants are lower limits of the constants based on the sensitivity of detecting inhibition.

of four substrate and three inhibitor concentrations. The remainder of the inhibitors were analyzed at one fixed substrate concentration and variable inhibitor concentrations. Inhibition constants for IAG-nucleoside hydrolase were established from full kinetic analysis with **V** and **X** as inhibitors. The results were consistent with competitive inhibition with respect to substrate. The remainder of the inhibition constants were characterized by titration of assay mixtures containing a fixed concentration of substrate with variable inhibitor concentrations. All kinetic data were fit to the equation for competitive inhibition, $v = k_{cat}A/(K_m(1 + I/K_i) + A)$, where v = initial reaction rate, k_{cat} = catalytic turnover number, A = substrate concentration, K_m = Michaelis constant, I = inhibitor concentration, and K_i = dissociation constant for the enzyme-inhibitor complex. For K_i determination at a fixed substrate concentration, this

Table 2: Comparison of Substrate and Transition State Isosteres for Nucleoside Hydrolases

| inhibitor | IU-nucleoside hydrolase | | IAG-nucleoside hydrolase | |
|--|-------------------------|------------------------|--------------------------|-----------|
| | K_i | K_m/K_i ^a | K_i | K_m/K_i |
| XIII  | 1600 μM | 0.07 | >30,000 μM ^b | <0.0006 |
| V  | 0.30 μM ^c | 370 | 180 μM | 0.1 |

^a The comparison is made for the inhibitors with inosine. The assays for IU-nucleoside hydrolase were in the presence of 58 μM nitrophenylriboside, using 50 mM Hepes, pH 8.0. ^b No significant inhibition was detected at 10 mM **XIII** using 560 μM nitrophenylriboside as substrate in 50 mM Hepes, pH 8.0. The lower limit of the K_i is based on the sensitivity of the assay. ^c Taken from Horenstein and Schramm (1993b) and included for comparison.

approach assumes that substrate and inhibitor compete for the catalytic site. In these cases, data were fit to the equation:

$$1/v = 1/k_{cat} + (K_m/k_{cat}A)(1 + I/K_i)$$

Inhibitors. Iminoribitol inhibitors were synthesized and purified according to the methods of Furneaux et al. (1997), characterized by NMR, dissolved in H₂O and stored at -20 °C. The compounds are enzymatically and chemically stable in H₂O and under conditions of the assay. IU-Nucleoside hydrolase is susceptible to slow-onset tight-binding inhibition under certain conditions (Horenstein & Schramm, 1993b; Boutellier et al., 1994). However, in the initial reaction rate conditions described here, only the rapidly reversible competition between substrate and inhibitor is being observed. Thus, the reported kinetic constants are dissociation constants which exclude slow-onset binding.

Synthesis of 1-deoxy-1-C-phenyl-β-D-ribofuranose (**XIII**, Table 2) was as described by Krohn et al. (1992). The product was purified by chromatography on silica gel and characterized by NMR.

RESULTS

Inhibition of IU-Nucleoside Hydrolase. The K_m value for the hydrolysis of inosine by IU-nucleoside hydrolase under the conditions described here is 111 ± 17 μM. The reaction exhibits a rapid-equilibrium random kinetic mechanism, making the K_m value approximately equal to the dissociation constant (Parkin et al., 1991). For nitrophenylribose, the K_m was 64 ± 6 μM. By comparison to inosine, all of the iminoribitols, including the unsubstituted **I**, bind more tightly to the enzyme than does inosine (Table 1). The relative affinities are conveniently expressed by the K_m/K_i ratio, since these are equivalent thermodynamic constants for enzymes which follow rapid equilibrium kinetic mechanisms. The ratio ranges from 14 for **II** to 3960 for **XII**. The most tightly bound inhibitors (**VI** to **XII**) incorporate the hydrophobic phenyl ring and a group which can serve as a hydrogen-bond donor or acceptor, preferably in the *para*-position. The rapid-equilibrium random mechanism and the intrinsic isotope effects of IU-nucleosidase have established that

N-ribosidic bond cleavage is the highest barrier on the reaction coordinate (Horenstein et al., 1991).

Inhibition of IAG-Nucleoside Hydrolase. The K_m value for IAG-nucleoside hydrolase of $18 \pm 1 \mu\text{M}$ for inosine approximates a thermodynamic dissociation constant because of the rapid-equilibrium random kinetic mechanism (Parkin, 1996). To confirm that *N*-ribosidic bond cleavage is rate-limiting, the $[1'\text{-}^3\text{H}]$ inosine kinetic isotope effect was measured for IAG-nucleoside hydrolase using the competitive isotope label method (Horenstein et al., 1991). The ^3H kinetic isotope effect of 1.067 ± 0.001 confirms that bond breaking occurs as part of the rate-limiting step in this reaction. Unlike IU-nucleoside hydrolase, the IAG-nucleoside hydrolase is poorly inhibited by free or substituted iminoribitols (Table 1). Of the twelve compounds in Table 1, only **X** binds as well as the preferred substrate, inosine, as indicated by the K_m/K_i ratios. The relative weak binding of these inhibitors results in K_m/K_i ratios of <0.04 to 1.5.

Inhibition of Nucleoside Hydrolases by an Iminoribitol Isostere. Inhibition of the IU-nucleoside hydrolase by substituted phenyliminoribitols has been attributed to the oxocarbenium ion mimic in the iminoribitol and to combined hydrophobic and hydrogen-bonding effects in the substituent (Horenstein & Schramm, 1993a,b; Parkin & Schramm, 1995). These effects can be further quantitated for the IU- and IAG-nucleoside hydrolases by comparing the inhibitory action of an isostere, 1-deoxy-1-*C*-phenyl- β -D-ribofuranose (**XIII**, Table 2) to the inhibition by phenyliminoribitol (**V**), and to the binding of inosine as the substrate.

For IU-nucleoside hydrolase, substitution of the phenyl group in carbon-linkage to ribose in place of hypoxanthine causes a 14-fold decrease in binding affinity relative to inosine. However in the IAG-nucleoside hydrolase, the same substitution results in a decline in affinity of >1670 -fold, and no binding can be detected at 10 mM of **XIII**. These observations indicate that Michaelis complex recognition comes primarily from the ribosyl and purine groups for the IU- and IAG-enzymes, respectively. The hydrophobic phenyl group provides some binding energy for the IU-enzyme but none for the IAG-enzyme. These observations are consistent with the more stringent purine group specificity for the IAG-enzyme.

Compared to the 300 nM and 180 μM inhibition constants observed with **V**, the isostere **XIII** gives values of 1.6 and >30 mM for the IU- and IAG-enzymes, respectively. Relative to ribose, the presence of the iminoribitol group causes a 5300-fold increase in inhibitor affinity for IU-nucleoside hydrolase, but only a 170-fold increase for the IAG-enzyme. These findings also support the stronger preference of the iminoribitol for the IU-nucleoside hydrolase.

DISCUSSION

Transition State Inhibitor Design for IU-Nucleoside Hydrolase. The transition state structure of IU-nucleoside hydrolase was previously determined by kinetic isotope effects, steady-state kinetic analysis, and spectroscopic studies of the enzyme (Horenstein et al., 1991; Horenstein & Schramm, 1993a,b; Parkin & Schramm, 1995; Deng et al., 1996). The hypothesis for the design of the inhibitors in Table 1 was that features of the enzymatic transition state, when incorporated into stable analogues, will provide efficient inhibitors (Wolfenden, 1972; Schramm et al., 1994).

Characteristics of the transition state established from the kinetic isotope effects include (1) oxocarbenium ion character in the ribosyl and (2) monoprotonation of the departing hypoxanthine to form (3) a neutral, planar hydrophobic leaving group. In attempts to mimic this transition state, iminoribitol provides the ribo-oxocarbenium mimic, and comparison of iminoribitol binding with that of its isostere (1-deoxyribose) indicated a >2000 -fold increase in binding affinity (Horenstein & Schramm, 1993b). The hydrophobic leaving group effect was originally established by the increased affinity of the phenyl group, which accounted for an additional 15-fold rapid-equilibrium binding inhibition relative to the unsubstituted iminoribitol and resulted in slow-onset inhibitor features (Horenstein, 1993b). A candidate for the enzymatic proton donor to the leaving group was established as His241 from the X-ray crystal structure and site-directed mutagenesis of this group; however, the position of the proton donor relative to the hypoxanthine leaving group in the transition state is ambiguous (Degano et al., 1996; Gopaul et al., 1996).

These features suggested that it might be possible to improve the hydrophobic group interactions between IU-nucleoside hydrolase and transition state inhibitors by positioning monosubstituted phenyl groups as leaving-group mimics to capture the additional energy of the proton donation which occurs to form the transition state complex. In addition, the use of substituents with different electrophilicity provides a means to explore the electronic nature of the enzymatic leaving group cavity in the transition state complex.

Interaction of the Inhibitors with IU-Nucleoside Hydrolase. The hypothesis that substituents which provide H-bonding sites and/or perturb the electronic configuration of the leaving group analogue will improve binding is supported by the data that all of the substituted iminoribitols **VI** through **XII** provide increased affinity relative to phenyliminoribitol (**V**). The binding affinity is substantial with all compounds binding at least a thousand-fold better than substrate in a rapid-equilibrium manner.³ The most tightly bound inhibitors contain electron donating substituents (**VII**, **IX**, and **X**) and/or have substituents which are hydrogen bond acceptors (**VI**, **VII**, **VIII**, **XI**, and **XII**). These relationships are explored in the Hammett plot of Figure 1. The inhibitors can be classified into two major groups. The solid line connects the $\text{p}K_i$ values for four inhibitors which show a conventional Hammett relationship, with slope of -0.55 . Within this group are the $-\text{OH}$ (**VII**) which can donate or accept hydrogen bonds, the phenyl group (**V**) which can neither accept nor donate a conventional hydrogen bond, the $p\text{-NH}_2$ group (**X**), which is only an H-bond donor when in conjugation with the aromatic ring, and the $m\text{-NO}_2$ substituent (**III**) which functions only as an H-bond acceptor. The relative affinity of these four inhibitors with diverse H-bonding capacity can be accommodated by a hydrogen bond between a group on the protein and the π -electrons of the phenyl ring. The electron donor groups, $p\text{-NH}_2$ and $-\text{OH}$ enrich the π -electron cloud, thus strengthening the bond to the electron-deficient H-bond donor from the protein. The

³ Compound **V** is known to induce slow-onset binding approximately 5-fold tighter than the initial K_i value. A similar mode of inhibition was observed with p -nitrophenylriboamidrazone (Boutellier et al., 1995). Similar studies are underway to characterize **VI**–**XII**.

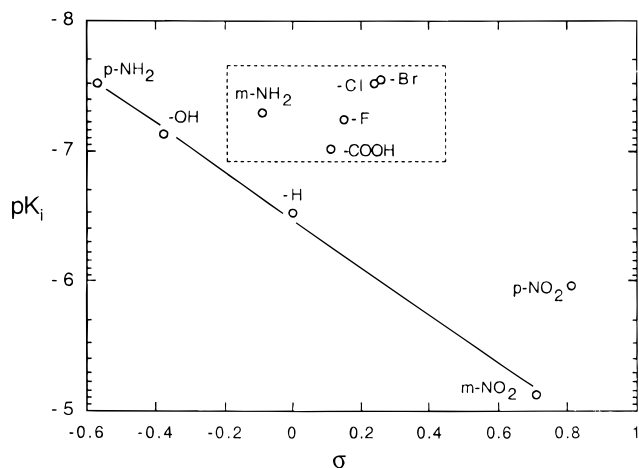


FIGURE 1: Hammett plot of the inhibition constants for the substituted phenyliminoribitols with IU-nucleoside hydrolase. Negative and positive σ values are assigned to electron-donating and electron-withdrawing substituents, respectively. The line is drawn by eye to the experimental data. The dashed box encloses a group of H-bonding substituents which bind tightly to IU-nucleoside hydrolase.

m-NO₂ depletes electron density from the π -cloud, thereby weakening the bond. These π -bonded systems have been described for hydrophobic-charged group interactions in protein structures (Burley & Petsko, 1988) where relatively weak π -bonds of 1–2 kcal/mol are formed between neighboring amino acids. In the case of the transition state inhibitors, the substituents are proposed to provide additional electron density and increase the range of energy available for this interaction. The 250-fold difference in K_i between *p*-NH₂ (**X**) and *m*-NO₂ (**III**) substituents corresponds to an energetic difference of 3.3 kcal/mol. Recent studies of the X-ray crystal structure of **X** with IU-nucleoside hydrolase are consistent with the formation of a π -electron bond in this position.⁴ In this structure, His82 is in the appropriate geometry to form a π -bonded interaction with the phenyl ring of **X** and His241 is in appropriate geometry for proton transfer to a purine in the catalytic site. Both interactions assist electron departure from the ribose to the purine leaving group and are logical contributions to catalysis and transition state binding energy for inhibitors.

All of the remaining substituent groups cause stronger binding to IU-nucleoside hydrolase than anticipated by the σ -value for a π -bonded interaction. The dashed rectangle in Figure 1 encloses five substituent groups, four of which can act as H-bond acceptors. These groups could accept hydrogen bonds from the enzyme, for example, through protonated His241 or His82. The halogen substituents are H-bond acceptors in the context of the transition state complex, since the bond can be formed in several directions relative to the plane of the phenyl ring. The carboxyl substituent can also accept H-bonds over a substantial portion of its geometry. In contrast, the *m*-NH₂ substituent of **IX** is unlikely to be an H-bond acceptor, since the conjugation of the amino group with the phenyl ring creates a planar structure which is confined to H-bond donation over a relatively narrow geometry. An explanation for the relatively strong inhibition by **IX** could be proposed to be H-bond donation to the unprotonated form of His241 or His82. An

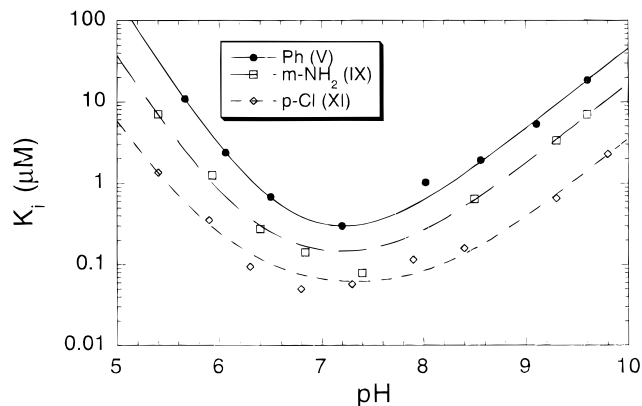


FIGURE 2: Inhibition constants for the interaction of **V**, **IX**, and **XI** with IU-nucleoside hydrolase as a function of pH. The solid circles are the data for phenyliminoribitol (**V**) (Parkin & Schramm, 1995), the open squares are for **IX**, and the open diamonds are for **XI**. The K_i values at each pH for **IX** and **XI** were determined at a single substrate concentration and multiple concentrations of inhibitor (see Materials and Methods). The K_m for IU-nucleoside hydrolase is independent of pH. The lines are drawn by fits of the data to the equation which assumes one protonation of the enzyme is required for inhibitor binding (K_b) and two subsequent protonations (K_a and K_d), abolish inhibitor binding [$K_{i, \text{obs}} = K_i(1 + H^+/K_a + K_b/H^+)(1 + H^+/K_d)$]. Protonation of the imino nitrogen of **V** has a pK_a of 6.5 (Horenstein & Schramm, 1993a), thus K_d was fixed at this value for the analysis. The limiting K_i values were 142, 88, and 46 nM for **V**, **IX**, and **XI**, respectively. The pK_a values for K_b were 7.5, 7.6, and 8.1, and those for K_a were 6.5, 6.1, and 5.4 for **V**, **IX**, and **XI**, respectively. Standard errors associated with the pK_a values were ± 0.1 –0.3.

alternative explanation would be favorable van der Waals interactions of the hydrophobic groups which are known to populate this portion of the catalytic site (Degano et al., 1996). Both a proton donor ($pK_a = 7.5$) and a proton acceptor ($pK_a = 6.6$) are involved in the formation of the transition state complex which requires unprotonated **V** (Parkin & Schramm, 1995). The pH-dependence of **IX** and **XI** binding is closely related to that of **V** (Figure 2). The explanation consistent with these results is for favorable van der Waals interactions between the enzyme **IX** and **XI**. The same ionization state of the enzyme which forms the inhibitor complexes for **V**, **IX**, and **XI** is required for k_{cat} [Figure 2 and Parkin and Schramm (1995)].

Inhibition of IAG-Nucleoside Hydrolase by Iminoribitols. The iminoribitol family of transition state inhibitors (Table 1) was designed from the features of the transition state for IU-nucleoside hydrolase. Use of **V** in metabolic studies with *C. fasciculata* revealed that iminoribitol-resistant pathways of nucleoside salvage are present (Estupiñán & Schramm, 1994). The resistant enzymes are purine-specific nucleoside hydrolases which have been purified both from *C. fasciculata* and from *T. brucei brucei*. The major nucleoside hydrolase activity in *T. brucei brucei* is the purine-specific IAG-nucleoside hydrolase (Parkin, 1996). The failure of the iminoribitol family to provide strong inhibition of the purine-specific enzymes, including the GI-nucleoside hydrolase from *C. fasciculata* (Estupiñán & Schramm, 1994) and the IAG-enzyme from *T. brucei brucei*, indicate fundamentally different catalytic mechanisms for the two enzymes. An indication in the diversity of the catalytic sites for these enzymes is the 39 000-fold difference in K_m/K_i values for IU- and IAG-nucleoside hydrolases with **XI**.

The monosubstituted phenyliminoribitols fail to induce transition state binding energies in the IAG-enzyme because

⁴ M. Degano et al., unpublished observations.

the majority of the transition state binding energy for this enzyme comes from leaving group activation rather than ribosyl activation towards the oxocarbenium transition state. These mechanistic differences are also indicated by the substrate specificity of the enzymes. Nitrophenylribose is a good substrate for enzymes which can activate the ribosyl toward the oxocarbenium ion, since the nitrophenylate anion is a good leaving group requiring no proton donation from the catalytic site. Enzymes which reach the transition state by activation of the leaving group are inefficient with nitrophenylribose since the nitro group is difficult to protonate at physiological pH values. Under the conditions used here, the k_{cat} for inosine is 28 and 34 s^{-1} while that with nitrophenylribose is 239 and 0.2 s^{-1} for the IU- and IAG-nucleoside hydrolases, respectively.⁵ Together with the inhibitor specificity of Table 1, the results indicate that these isozymes have distinct catalytic mechanisms leading to structurally distinct transition states.

Comparison of the pH Profiles for IU- and IAG-Nucleoside Hydrolase. Activation of purine leaving groups occurs in acid-catalyzed solvolysis by multiple protonation of ring nitrogens (Garrett & Mehta, 1972). Enzymes which require the transfer of multiple protons to reach the transition state would be expected to show these enzymatic groups in the pH profiles for k_{cat} . Published pH profiles for the k_{cat} values of IU- and IAG-nucleoside differ in that the IU-enzyme requires one proton donor ($\text{p}K_{\text{a}}$ 9.1) and one proton acceptor ($\text{p}K_{\text{a}}$ 7.1) to achieve catalysis (Parkin & Schramm, 1995). In contrast, the IAG-enzyme appears to require two proton donors with $\text{p}K_{\text{a}}$ 8.8 and a third at $\text{p}K_{\text{a}}$ 6.5 to be protonated for full catalytic activity (Parkin, 1996). Thus, catalysis by IU-nucleoside hydrolase can be classified as acid–base catalysis, while the three proton donations for IAG-nucleoside hydrolase indicate acid catalysis.

Energetics of Transition State Stabilization. The energetics of ribosyl activation relative to leaving group activation can be evaluated for IU- and IAG-nucleoside hydrolases by a comparison of the (1) relative rates of chemical and enzymatic hydrolysis with inosine as substrate, (2) the same parameters with nitrophenylribose as substrate, (3) relative affinity of phenyliminoribitol (**V**) and its isostere (**XIII**), and (4) the relative affinities of the transition state analogues of Table 1. The $\Delta\Delta G$ for the energy of activation for bond cleavage in nitrophenylribose is estimated to be 13 kcal/mol based on the pH dependence of the reaction in H_2O . In contrast, the $\Delta\Delta G$ energy of activation for purine *N*-riboside bond cleavage for inosine is 17.7 kcal/mol based on the same criterion (Gopaul et al., 1996). Together with assignment of -4.6 kcal/mol to leaving group activation with the IU-nucleoside hydrolase, the energy of activation applied to the ribosyl of inosine or nitrophenylribose is -13.1 kcal/mol (Figure 3). The k_{cat} for inosine is similar for both IU- and IAG-nucleoside hydrolases and both have bond cleavage as rate-limiting steps. Therefore both enzymes apply approximately -17.7 kcal/mol to lower the energy of activation. However the IAG enzyme is inefficient with nitrophenylribose as substrate, with $k_{\text{cat}}(\text{IU})/k_{\text{cat}}(\text{IAG}) = 980$, a

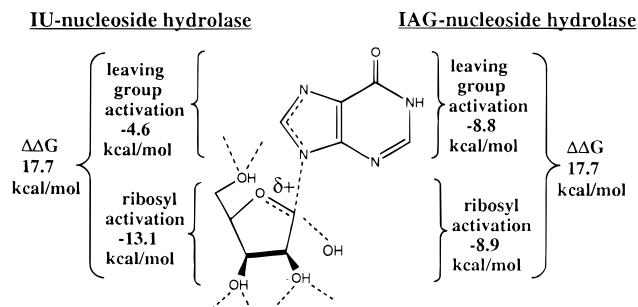


FIGURE 3: Energetics of *N*-ribosidic hydrolysis of inosine by IU-nucleoside hydrolase and IAG-nucleoside hydrolase. Values on the far left and right correspond to the total value by which the enzymes lower the energy of activation for inosine solvolysis at neutral pH values ($k_{\text{enzyme}}/k_{\text{chem}}$ for inosine). Values on the inner left correspond to the relative energies for leaving group and ribosyl activation, respectively for the IU-enzyme. They are based on mutational studies with H241A, proton donor to the leaving group (Gopaul et al., 1996). Values on the inner right correspond to the same functions for the IAG-enzyme. The values are estimated from $[k_{\text{cat}}(\text{inosine})/k_{\text{cat}}(\text{nitrophenylribose})]$ using the kinetic constants from the results presented here and may not be valid for other substituents. The inosine is indicated at the transition state where oxocarbenium ion character is developed in the ribose. The unusual *syn*-conformation of the 5'-hydroxyl is predicted from kinetic isotope effects (Horenstein & Schramm, 1993a). The incipient water nucleophile is shown as an $-\text{OH}$, and the interactions of the 2'-, 3'-, and 5'-hydroxyls with protein are indicated by the dashed lines.

change of 4.2 kcal/mol in energy of activation. Since this substrate reacts primarily by ribosyl activation, it can be concluded that the ability of the IAG-enzyme to activate the ribosyl is 4.2 kcal/mol less than that of the IU-enzyme. Thus of the -17.7 kcal/mol energy of activation applied by the IAG-enzyme -8.8 is leaving group activation while the remaining -8.9 kcal/mol is ribosyl activation. This energy of activation analysis is independent of the data for transition state inhibitor information. However the difference between -13.1 and -8.9 kcal/mol for ribosyl activation indicates that ribooxocarbenium analogues should bind approximately 4.2 kcal/mol less favorably to the IAG-enzyme than the IU-enzyme. Comparison of the inhibitors in Table 1 for the IU- and IAG-enzymes generally support this proposal, since all of the inhibitors bind more tightly to the IU- than the IAG-nucleoside hydrolase (Table 1). Perfect quantitation of these energies cannot be achieved with transition state inhibitors, since they are imperfect mimics of the nonequilibrium bond lengths of the transition state.

The isostere data of Table 2 demonstrate that both enzymes prefer the iminoribitol to the deoxyribosyl group, but the affinity differs significantly. The difference in affinity relative to substrate $[K_{\text{m}}/K_{\text{i}} (\text{IU-enzyme})]/[K_{\text{m}}/K_{\text{i}} (\text{IAG-enzyme})]$ is 3700, equivalent to 5.0 kcal/mol more binding energy for phenyliminoribitol to the IU- than the IAG-enzyme, again consistent with the energetics profile of Figure 3.

Catalytic Mechanisms for the Nucleoside Hydrolases. Three demonstrated chemical mechanisms for solvolysis of nucleosides and nucleoside derivatives include (1) acid-catalyzed solvolysis by protonation of the leaving group, (2) base-catalyzed ionization of the ribosyl hydroxyls, and (3) neighboring-group stabilization of the oxocarbenium ion which characterizes the transition states of these reactions. Acid-catalyzed solvolysis for purine nucleosides proceeds most rapidly from the dicationic, diprotonated purine (Garrett & Mehta, 1972). The positive leaving group withdraws

⁵ The value for the substrate activity of nitrophenylribose with IAG-nucleoside hydrolases published previously (Mazzella et al., 1996) was 0.8 compared with the value of 0.2 obtained here. The use of more highly purified enzyme for the work reported here may account for this difference.

electrons from the *N*-ribosidic bond, creating a distributed positive charge on the ribosyl oxocarbenium ion at the transition state (Mentch et al., 1987; Horenstein & Schramm, 1993a,b). 2'-Deoxynucleosides react more rapidly under acid-catalyzed solvolysis, since they lack the electron-rich hydroxyl which contributes to the stability of the *N*-ribosidic bonding electrons. Base-catalyzed ionization of the ribosyl hydroxyls has been proposed for the alkaline solvolysis of NAD⁺ and its derivatives (Handlon et al., 1994). Positioning of anionic groups near the ribosyl of nucleosides aids formation of the cationic transition state and has been demonstrated in model studies (Cherian et al., 1990). A fourth mechanism can be included for enzymatic reactions and involves metal-ion activation of the attacking water nucleophile (Degano et al., 1996).

N-Ribohydrolases have been proposed to use all four mechanisms. The enzymes activate a specific water nucleophile since solvolysis in the presence of mixed solvent nucleophiles permits only water molecules to react (Parkin et al., 1991). The transition state properties of AMP nucleoside hydrolase and IU-nucleoside hydrolase indicate a protonated leaving group, activation of a specific water nucleophile, and stabilization of the ribosyl oxocarbenium (Mentch et al., 1987; Horenstein et al., 1991). The X-ray crystal structure of IU-nucleoside hydrolase supports these mechanisms and implicates the groups responsible for all three catalytic forces. A bound metal ion activates the water nucleophile and His82 and/or His241 protonates the leaving group (Degano et al., 1996). This mechanism correlates with the inhibition constants of Table 1. None of the compounds is capable of the multiple, geometrically distributed proton-accepting properties proposed for purine nucleosides to stabilize the transition state for IAG-nucleoside hydrolase, and thus they are poor inhibitors for this isozyme.

Summary. The iminoribitol transition state inhibitors are specific for the ribo-oxocarbenium ion stabilizing mechanism of IU-nucleoside hydrolase. They bind poorly to the IAG-enzyme which derives more of its activation energy from leaving-group interactions. These findings demonstrate the feasibility of designing isozyme-specific inhibitors based on differences in catalytic mechanism and transition state structure.

ACKNOWLEDGMENT

The authors thank Massimo Degano for helpful discussions to correlate protein structure and inhibitor affinity for IU-nucleoside hydrolase.

REFERENCES

- Boutellier, M., Horenstein, B. A., Semenyaka, A., Schramm, V. L., & Ganem, B. (1994) *Biochemistry* 33, 3994–4000.
- Burley, S. K., & Petsko G. A. (1988) *Adv. Protein Chem.* 39, 125–189.
- Cherian, X. M., Van Arman, S. A., & Czarnik, A. W. (1990) *J. Am. Chem. Soc.* 112, 4490–4498.
- Degano, M., Gopaul, D. N., Scapin, G., Schramm, V. L., & Sacchettini, J. C. (1996) *Biochemistry* 35, 5971–5981.
- Deng, H., Chan, A. W.-Y., Bagdassarian, C. K., Estupiñán, B., Ganem, B., Callender, R. H., & Schramm, V. L. (1996) *Biochemistry* 35, 6037–6047.
- Dewey, V. C., & Kidder, G. W. (1973) *Arch. Biochem. Biophys.* 157, 380–387.
- Estupiñán, B., & Schramm, V. L. (1994) *J. Biol. Chem.* 269, 23068–23073.
- Furneaux, R. H., Limberg, G., Tyler, P. C., & Schramm, V. L. (1997) *Tetrahedron* (in press).
- Garrett, E. R., & Mehta, P. J. (1972) *J. Am. Chem. Soc.* 94, 8532–8541.
- Gopaul, D. N., Meyer, S., Degano, M., Sacchettini, J. C., & Schramm, V. L. (1996) *Biochemistry* 35, 5963–5970.
- Hammond, D. J., & Gutteridge, W. E. (1984) *Mol. Biochem. Parasitol.* 13, 243–261.
- Handlon, A. L., Xu, C., Muller-Steffner, H. M., Schuber, F., & Oppenheimer, N. J. (1994) *J. Am. Chem. Soc.* 116, 12087.
- Horenstein, B. A., & Schramm, V. L. (1993a) *Biochemistry* 32, 7089–7097.
- Horenstein, B. A., & Schramm, V. L. (1993b) *Biochemistry* 32, 9917–9925.
- Horenstein, B. A., Parkin, D. W., Estupiñán, B., & Schramm, V. L. (1991) *Biochemistry* 30, 10788–10795.
- Horenstein, B. A., Zabinski, R. F., & Schramm, V. L. (1993) *Tetrahedron Lett.* 34, 7213–7216.
- Krohn, K., Heins, H., & Wielckens, K. (1992) *J. Med. Chem.* 35, 511–517.
- Matthews, D. A., Bolin, J. T., Burrige, J. M., Filman, D. J., Volz, K., Kaufman, B. T., Beddell, C. R., Champress, J. N., Stammers, D. K., & Kraut, J. (1985) *J. Biol. Chem.* 260, 381–391.
- Mazzella, L. J., Parkin, D. W., Tyler, P. C., Furneaux, R. H., & Schramm, V. L. (1996) *J. Am. Chem. Soc.* 118, 2111–2112.
- Mentch, F., Parkin, D. W., & Schramm, V. L. (1987) *Biochemistry* 26, 921–930.
- Miller, L. H. (1992) *Science* 257, 36–37.
- Miller, R. L., Sabourin, C. L. K., Krenitsky, T. A., Berens, R. L., & Marr, J. J. (1984) *J. Biol. Chem.* 259, 5073.
- Parkin, D. W. (1996) *J. Biol. Chem.* 271, 21713–21719.
- Parkin, D. W., & Schramm, V. L. (1995) *Biochemistry* 34, 13961–13966.
- Parkin, D. W., Horenstein, B. A., Abdulah, D. A., Estupiñán, B., & Schramm, V. L. (1991) *J. Biol. Chem.* 266, 20658–20665.
- Schramm, V. L., Horenstein, B. A., & Kline, P. C. (1994) *J. Biol. Chem.* 269, 18259–18262.
- Wolfenden, R. (1972) *Acc. Chem. Res.* 5, 10–18.

BI962319V